Streptococcal protein fog: A novel matrix adhesin interacting with colagen I in vivo.

Nitsche, Patric; Linge, Helena; Frick, Inga-Maria; Mörgelin, Matthias

Published in:
Journal of Biological Chemistry

DOI:
10.1074/jbc.M506776200

2006

STREPTOCOCCAL PROTEIN FOG: A NOVEL MATRIX ADHESIN INTERACTING WITH COLLAGEN I *IN VIVO*[*]

D. Patric Nitsche*, Helena M. Johansson*, Inga-Maria Frick†, and Matthias Mörgelin†
From the Department of Clinical Sciences, Section for Clinical and Experimental Infectious Medicine, Biomedical Center, Lund University, S-22184 Lund, Sweden

Running Title: Protein FOG Interacts With Collagen I In Vivo

* D.P.N. and H.M.J. contributed equally to this work

† Address correspondence to: Inga-Maria Frick, Department of Clinical Sciences, Section for Clinical and Experimental Infectious Medicine, Biomedical Center, Lund University, S-22184 Lund, Sweden, Tel. +46-46-2228569; Fax. +46-46-157756, E-Mail: inga-maria.frick@med.lu.se, or Matthias Mörgelin, Department of Clinical Sciences, Section for Clinical and Experimental Infectious Medicine, Biomedical Center, Lund University, S-22184 Lund, Sweden, Tel. +46-46-2220741; Fax. +46-46-157756, E-Mail: matthias.morgelin@med.lu.se.

Group G *streptococcus* (GGS) is a human pathogen of emerging clinical significance. It causes skin and soft tissue infections, occasionally resulting in life threatening conditions such as sepsis and necrotizing fasciitis. We recently identified FOG, a novel surface protein of GGS with fibrinogen-binding and immune evasion properties. Here we investigated the role of FOG in streptococcal primary adhesion to host tissue. A FOG-expressing clinical isolate adhered considerably more efficient to human skin biopsies *ex vivo* and to the murine dermis *in vivo,* than a FOG-deficient strain. Scanning and transmission electron microscopy of skin specimens exhibited that this property was assigned to the ability of FOG to interact with collagen I, a major interstitial component of the dermis. Overlay experiments with human skin extracts and radiolabeled FOG, followed by matrix-assisted laser desorption/ ionisation time of flight mass spectrometry (MALDI-TOF-MS) analysis identified both the α1- and α2-chain of collagen I as targets for FOG. Transmission electron microscopy of the molecular complexes revealed thread-like FOG molecules binding via their NH_2-termini to distinct sites on collagen I monomers and fibrils. The results demonstrate that FOG is crucial for GGS adhesion *in vivo*, implying a pathogenic role for this surface protein.

Streptococcus dysgalactiae equisimilis, a group G streptococcus (GGS), can cause mild infections like pharyngitis and more severe skin infections such as erysipelas and abscess formation. Deep soft tissue infections may result in life threatening conditions such as sepsis and necrotizing fasciitis (for references see 1). While certain cases of rheumatic fever have been linked to pharyngeal carriage of GGS (2), primary infections of the skin with these pathogens were often found to precede serious invasive conditions and bacteremia (3). Thus, the skin is to be considered an important site of entry. The clinical relevance of skin infections caused by GGS is underlined by epidemiological reports indicating that GGS are at least as frequent as group A streptococci (GAS) in such disease (4,5).

Primary adhesion to the host tissue is a crucial initial step in bacterial infection. The firm interaction enables the bacteria to persist at the site of infection and subsequently colonize specific locations in the tissue. Certain streptococcal surface components with the potential to adhere to host tissues have been identified previously (for references see 6,7). For GAS a mechanism has been postulated in which lipoteichoic acid acts in concert with other bacterial surface proteins to facilitate adhesion to host cells (8-10). Frequently fibronectin has a key function by bridging bacterial adhesins and eukaryotic integrins (11-15). Interestingly, some of the M proteins, which are important multifunctional virulence factors of GAS, meet the criteria of adhesins (for references see 6,7). As an example, M1 protein involves both fibronectin and laminin in adhesion to human lung epithelial cells (16).

A recent study indicates that the majority of GAS strains use the adhesin SfbI to recruit collagen types I and IV via surface bound fibronectin (17). Alternative mechanisms for

collagen binding, such as a direct interaction with an M protein of the M3 serotype or binding via a capsule of hyaluronic acid, as seen for an M18 strain, have been published recently (18). *Staphylococcus aureus* has recently been reported to express the adhesin CNA to directly bind collagen in a mouse model of septic arthritis (19).

Despite the clinical and epidemiological importance and the occasionally dramatic pathogenesis of skin infections with GGS, molecular mechanisms for colonization of human skin by these pathogens are still elusive. A fibronectin-binding protein of GGS, GfbA, has been described earlier as a mediator of adhesion to human fibroblasts. The encoding gene was detected in 36% of tested strains, suggesting that there might be other tissue-specific adhesins expressed by these pathogenic streptococci (20). The recently discovered GGS surface protein FOG has been shown to share sequence homology and structural similarity with M-like proteins of other streptococci. Using primers from the signal sequence and the cell wall anchoring domain of FOG, a PCR product corresponding to the 1.8 kbp FOG gene was generated in 97% of examined clinical isolates of GGS (21).

In the present study, we provide evidence that GGS adhere to collagen I fibrils of the dermis *in vivo* employing protein FOG as an adhesin. Binding sites essential for this interaction were identified in the NH_2-terminal part of FOG and on two distinct positions on the collagen I triple helix. Taken together, the data demonstrate that this surface protein is an important virulence determinant with the potential to trigger streptococcal pathogenesis *in vivo*.

MATERIALS AND METHODS

Bacterial strains – Human clinical isolates of GGS were collected at the Department of Clinical Microbiology, Lund University Hospital, Sweden. Strains G10, G11, G14, and G19 were joint isolates, G30 and G35 were isolated from wounds and G41 and G148 were throat specimens. Bacteria were cultured in Todd-Hewitt broth (TH; Difco) at 37°C and 5% CO_2. Strain G148 lacks the *fog* gene (21) and served as a negative control.

Recombinant Proteins – Purification of the FOG variants was performed as described (21). FOG 1-C (amino acid residues 1- 493) lacks the COOH- terminal D-domain including the bacterial cell wall anchoring LPXTG-motif and FOG 1-B covers the NH_2-terminal 278 residues (Fig. 3E). The recombinant proteins carry an NH_2-terminal GST-tag used for protein isolation.

Radiolabeling and Bacterial Binding Assay – Collagen I from calf skin (Vitrogen Inc.), human plasma fibronectin (Sigma-Aldrich) and FOG 1-C were radiolabeled with ^{125}I using IODO-BEADS (Pierce). The labeling reactions were carried out on ice for collagen I and at room temperature for the other proteins using 20 μg of protein in 30 mM phosphate (KH_2PO_4/Na_2HPO_4), 120 mM NaCl, pH 7.4 (PBS) and 5 min initial incubation. Unbound iodine was removed on a PD10-column (Amersham Biosciences). ^{125}I-labeled proteins were bound to streptococcal cells as described earlier (22). All reactions were performed on ice.

Human Skin Samples – Punch biopsies (4 mm diameter) of human skin were obtained in connection with skin transplant surgery. Informed consent was obtained from the patients. The Ethics Committee at Lund University approved the use of this material (LU 509-01, LU 708-01).

Ligand blot and slot blot – Human skin components were extracted by boiling in 20% SDS for 20 min. Solubilized proteins were separated by SDS-PAGE on a 3-12% gradient gel and stained with Coomassie Brilliant Blue or electro-blotted onto a PVDF membrane (Immobilon, Millipore). The membrane was washed twice for 30 min in blocking buffer (PBS containing 0.25% Tween 20 and 2% bovine serum albumin), incubated with ^{125}I-FOG 1-C overnight at 4ºC and washed three times for 20 min in blocking buffer. Signals of bound ligand were detected using the Fuji Imaging System. Bands corresponding to the signals on the blot were excised from the Coomassie-stained gel and prepared for mass spectrometry. Collagen I denatured with guanidine hydrochloride, and non-denatured collagen I were applied directly onto a PVDF membrane using the Milliblot-D system (Millipore). Membranes were blocked, washed, and incubated with radiolabeled probe as described above.

Mass Spectrometry – Excised gel bands were washed in water and destained with 40% acetonitrile in 25 mM NH_4HCO_3, pH 7.8 (Buffer A). The gel pieces were vacuum-dried and rehydrated in 10-20 μl of 10 mM dithiothreitol

(55°C, 30 min). Excess liquid was removed and the reduced proteins were alkylated using 10-20 µl of 55 mM iodoacetamide (20°C, 30 min). Samples were then washed with buffer A and vacuum-dried. Rehydration and overnight incubation at 37°C with 10-20 µl of buffer A containing sequencing grade trypsin (25 ng/ml, Promega) ensued digestion into peptides, which were extracted in 10 µl of 2% trifluoroacetic acid and purified using C18 Ziptips (Millipore). Precrystallized 2,5-dihydroxybenzoic acid was provided on an Anchorchip target (Bruker Daltonik GmbH). The purified peptides were eluted onto this matrix using 50% acetonitrile, 0.1% trifluoroacetic acid and allowed to co-crystallize. Spectrometry was carried out on a Bruker Reflex III matrix-assisted laser desorption/ionization time-of-flight (MALDI-TOF) mass spectrometer operated at an acceleration voltage of 26 kV in the positive ion/delayed extraction mode and detection in the reflector mode. Autolysis fragments of trypsin were used for external calibration of the spectra that were summed of 75-100 single-shot measurements each. Proteins were identified using the Web tool ProFound (23). The settings accounted for a complete alkylation of the cysteine-residues, partial oxidation of methionine and hydroxylation of lysine and proline. Missed cuts were excluded. Other parameters were used in their default settings.

Surface Plasmon Resonance Measurements – Interactions were studied in the BIAcore 2000 system (BIAcore AB) using 10 mM HEPES, 100 mM NaCl, pH 7.4 as running buffer. A CM5 sensor chip was activated by a 4 min injection of 0.05M N-hydroxysuccinimid, 0.2 M N-ethyl-N-(3-dimethylaminopropyl)-carbodiimide hydrochloride in water. Collagen I from calf skin (Boehringer Mannheim) was diluted in 15 mM NaAc, pH 5.3, to a final concentration of 15 µg/ml. Injection of 5 µl at a flow rate of 5 µl/min lead to immobilization of 400 response units (RU) of collagen I. Residual reactive groups were inactivated by 6 min injection of 1 M ethanolamine, 0.1 M $NaHCO_3$, 0.5 M NaCl, 5 mM EDTA, pH 8.0. Interaction measurements with FOG, FOG 1-C, FOG 1-B, and GST, respectively, were performed at a flow rate of 50 µl/min. No mass transfer effects were detected. Surface regeneration was achieved by injection of a 30 s pulse of 0.2% SDS in water. Data were analysed using the BIAevaluation 3.0 software and shown curves represent the difference between the signal of the collagen-coupled surface and a deactivated control surface devoid of protein. They were further corrected by subtraction of the curve obtained after injection of buffer alone.

Bacterial Binding to Human Skin Sections – Skin biopsies were fixed in PBS containing 4% formaldehyde (18 h, 4ºC) and processed for paraffin sectioning. Deparaffinized and rehydrated 5 µm sections were incubated with bacterial suspensions (2×10^9 c.f.u./ml) in PBST for 1 min, 15 min, 30 min, 1 h or 2 h at room temperature. Prior to experimental colonization conditions, 1h of primary adhesion was carried out. After removing non-bound bacteria with PBST, a drop of TH-medium was placed on the sections and the slides were incubated at 37ºC, 5% CO_2 for 5 h to allow bacterial multiplication. In both types of experiments non-bound bacteria were finally removed by extensive washing with PBST. The samples were fixed in PBS containing 4% formaldehyde and prepared for light microscopy. Samples for scanning electron microscopy were fixed and processed as described below.

Bacterial Colonization of Human Skin Biopsies – Skin biopsies were incubated with bacteria (2×10^9 c.f.u./ml) in PBST for 1h at room temperature. After removal of non-bound bacteria by washing three times with PBST, the infected skin was cultivated for 24 h in DMEM (Gibco BRL) at 37ºC, 5% CO_2. The samples were washed three times in PBS and specimens were either fixed in PBS containing 4% formaldehyde prior to light microscopy, or prepared for scanning electron microscopy as described below.

Primary adhesion to the collagen matrix of human fibroblasts – Bacteria were grown in TH to early stationary growth phase, washed three times with PBS and resuspended in PBS to 2×10^9 c.f.u./ml. Human foreskin fibroblasts were cultured in 24-well tissue culture plates (Nunc) in MEM supplemented with 10% FBS, 100 U/ml penicillin, 100 µM streptomycin and 0.1 mM L-glutamine. Specimens for scanning electron microscopy were cultured under identical conditions on coverslips placed at the bottom of the wells. All reagents were from GibcoBRL. When cells approached confluence, a daily dose of ascorbic acid (25 µg/ml) was added for three days to stimulate the expression of collagen networks. Cell monolayers were washed with PBS, incubated with streptoccci (6×10^8

c.f.u./well) for 1 h at 37°C, 5% CO_2 and non-bound bacteria were removed with PBS. Analysis of adherent bacteria was either performed by determining c.f.u. as described (24), or by scanning electron microscopy.

Primary adhesion to the murine dermis in vivo – Female Balb/c mice of 6-8 weeks were anesthetized with isoflurane. Groups of three mice each received a subcutaneous dorsal injection of 6 x 10^8 c.f.u. G41 or G148. The area of injection was marked with a pencil for later identification. After 30 min the animals were sacrificed and the marked area was excised. For determination of adherent bacteria skin pieces were washed with PBS and homogenized in a volume of 400 µl PBS, using a Multi-Gen 7 homogenizer (Pro Scientific Inc. Monroe, CT, USA). Samples were vortexed, diluted and plated in duplicate on blood agar plates. Plates were incubated overnight at 37°C and the number of c.f.u. was counted. For determination of contaminating normal flora one mouse was injected with PBS alone and treated as above. In parallel, skin samples were prepared for examination by scanning electron mciroscopy.

The animal experiments were approved by the regional ethical committee for animal experimentation (permit number M294-03).

Light Microscopy – For light microscopy of colonized skin biopsies 5-µm paraffin sections were stained with Mayers Hematoxylin (Histolab AB) and Eosin Y (Surgipath Inc.). Alternatively, using the affinity of protein G to goat-IgG, the bacteria were detected with the Vectastain ABC Elite kit (Vector Laboratories Inc.) and subsequent staining with a DAB kit (Vector Laboratories Inc.), following the manufacturer's instructions. The samples were examined in a Carl Zeiss Axioplan 2 imaging e microscope. Digital images were acquired using a Carl Zeiss AxioCam HR camera and the software Axiovison 3.1 (Zeiss).

Scanning Electron Microscopy – Deparaffinized skin sections on glass slides were incubated with bacteria as described above. The whole slide was fixed in 4% formaldehyde, 2.5% glutaraldehyde in PBS, for two hours at 4°C. Fixed specimens were dehydrated for 10 min at each step of an ascending ethanol series and critical point dried in a Balzers critical point dryer in liquid carbon dioxide using absolute ethanol as intermediate solvent. The glass slides were cut into appropriate pieces with a diamond knife, mounted on aluminium stubs and coated with a 30 nm thick layer of gold. They were examined in a Jeol J-330 scanning electron microscope at an acceleration voltage of 5 kV and a working distance of 10 mm.

Transmission Electron Microscopy – Skin biopsies incubated with bacteria (see above) were fixed, embedded and sectioned with a diamond knive as previously described (21). The structure of FOG constructs and complexes thereof with collagen I was analysed by mica sandwich squeezing/rotary shadowing (25). Complexes between FOG, labelled with colloidal gold (26), and reconstituted collagen I fibrils were visualized by negative staining as described (27). To prepare collagen I fibrils an acidic solution of collagen I from fetal calf skin (3 mg/ml, Boehringer Mannheim) was neutralized with PBS to a final concentration of 25 µg/ml. Reconstitution of fibrils was carried out for 24 h at 37°C. Sample concentrations were usually in the range of 10–20 µg/ml in 50 mM Tris-HCl, 0.15 M NaCl, pH 7.4 (TBS). Collagen I fibrils and gold-labeled FOG were incubated in TBS buffer for 30 min at 4°C. Specimens were observed in a Jeol JEM 1230 electron microscope operated at 60 kV accelerating voltage. Images were recorded with a Gatan Multiscan 791 CCD camera.

RESULTS

GGS expressing FOG adhere to human dermis ex vivo – The FOG expressing GGS strain G41 was compared to the FOG-deficient strain G148 (21) for the ability to adhere to and subsequently colonize human dermis *ex vivo* (Fig. 1). Bacteria were allowed to adhere to thin sections of human skin biopsies on glass slides. For subsequent colonization the adhered bacteria were multiplied by incubation on the slides with culture medium. As shown by light microscopy G41 colonies adhered to the fibrous matrix of the dermis, whereas binding of G148 was considerably less pronounced (Fig. 1A). This was confirmed by scanning electron microscopy of infected skin sections at higher resolution (Fig. 1B). Large numbers of colonies of G41 bound to fibrillar structures in the dermis (arrowheads). In contrast, only few colonies of G148 could be detected. Fresh human skin biopsies were also infected with G41 or G148, followed by cultivation to simulate colonization of the tissue. By light microscopy the formation of large colonies in the dermis was obvious (arrowheads),

where colonization by strain G41 was much more pronounced as compared to G148 (Fig. 1C). Scanning electron microscopy (Fig. 1D) demonstrated a frequent intimate association of G41 colonies with fibrillar networks (insert), which was observed to a much lesser extent for G148.

FOG binds to collagen I α1- and α2-chains of skin extracts – To identify skin components serving as substrates for FOG we set up ligand blot experiments (Fig. 2A). The FOG 1-C fragment, lacking the COOH-terminal membrane anchor domain (Fig. 3E), was used to minimize potential self-aggregation by hydrophobic interactions. Human skin biopsies were extracted with SDS, separated by SDS-PAGE using bovine collagen I as a standard, and transferred to a PVDF membrane. Interestingly, radiolabeled FOG 1-C bound only to a few discrete bands of the skin extract with apparent molecular weights of 129, 141 and 207 kD, respectively (Fig. 2A, *Blot*). In the control lane FOG 1-C interacted with the α1- and α2-chains as well as β-, γ- and slower migrating fragments of bovine collagen I. Comparison with the Coomassie-stained gel showed that the bands exhibited a similar migration pattern as the α1- and α2-chains and the β-fragment of bovine collagen I (Fig. 2A, *Stain*).

Corresponding bands on the Coomassie-stained gel were excised, digested with trypsin and analyzed by MALDI-TOF-MS. The obtained peptide fingerprints identified all bands as collagen I (Table I). The data evaluation took into account the hydroxylation of proline and lysine residues characteristic for collagens. This led to uncertainties in the exact peptide assignment of the two homologue collagen I α-chains. However, the combination of the MALDI-TOF fingerprint data and the migration pattern in SDS-PAGE (Fig. 2; for identification of the bands see (22)) led to the assignment presented in Table I, concluding that both collagen I α-chains are targets for FOG.

To test the influence of collagen denaturation, occuring in SDS-PAGE, on the FOG-collagen interaction the binding of FOG 1-C to non-denatured and to guanidine hydrochloride-denatured bovine collagen I was examined in a slot blot experiment. Radiolabeled FOG 1-C bound to both collagen preparations in a similar concentration-dependent manner (Fig. 2B).

FOG binds to the collagen I triple helix in surface plasmon resonance experiments - GST-tagged recombinant full-length FOG, as well as the shorter variants FOG 1-C and FOG 1-B, were tested for binding to immobilized collagen I. All fragments exhibited a dose-dependent binding to collagen I (Fig. 3A-C), while the GST-tag alone did not bind (Fig. 3D). Binding curve fits based on the 1:1-model of Langmuir revealed apparent dissociation constants of 8×10^{-11} M for FOG, 4×10^{-10} M for FOG 1-C, and 3×10^{-10} M for FOG 1-B, respectively. Binding of the FOG 1-B fragment localized the site of collagen binding to the NH_2-terminal half of FOG (Fig. 3E).

Structural characterization of FOG – Visualization of GST-tagged recombinant full-length FOG and its truncated variants FOG 1-C and FOG 1-B by mica sandwich squeezing/rotary shadowing and transmission electron microscopy revealed thread-like particles with a globular terminal domain (Fig. 3F). The major portion of the globular domain is formed by the NH_2-terminal GST-tag as demonstrated by electron microscopy of recombinant GST alone. The thread-like structures are formed by FOG (55 ± 5 nm), FOG 1-C (41 ± 5 nm), and FOG 1-B (22 ± 3 nm), respectively. Their length correlates well with the number of amino acids (Fig. 3E), resulting in averages of 1.0 ± 0.1 Å, 0.8 ± 0.1 Å, and 0.8 ± 0.1 Å for the axial distances between vicinal amino acids, respectively. In summary the different recombinant proteins consist of an NH_2-terminal globular GST-tag and a protruding thread-like structure formed by the FOG-moiety that is more tightly packed than expected for an ideal α-helix (1.5 Å axial distance).

FOG binds to distinct sites on the collagen I triple helix – The interaction between FOG and collagen I was visualized by transmission electron microscopy after mica sandwich squeezing/rotary shadowing (Fig. 4A). Large fields of FOG molecules in association with the 300 nm long collagen I molecules became apparent. The contact between FOG and collagen I occurred at the very NH_2-terminal portion of FOG, which is marked by the globular GST-tag. Consistent with the surface plasmon resonance measurements, an interaction between GST alone and collagen I was not observed (data not shown). Therefore we concluded that the site of interaction resided in the NH_2-terminal of the FOG-moiety, without any contribution by the GST-tag. On the collagen I triple helix two

distinct binding sites for FOG were found (Fig. 4B). As pepsin-extracted collagen I was used we could not distinguish between NH_2- and COOH-terminal. However, collagen molecules were found with both binding sites occupied by FOG (Fig. 4B, lower panel). They allowed defining the relative position of the two binding positions, which are located on one tip and at 235 nm distance on the 300 nm long triple helix (Fig. 4C). Additional binding sites were not observed. The truncated recombinant variants FOG 1-C and FOG 1-B exhibited the same interactions with collagen I (data not shown).

FOG binds to distinct sites on collagen I fibrils – For a more detailed understanding of GGS adhesion to dermis collagen networks *in situ*, complexes between FOG and reconstituted collagen I fibrils were visualized by electron microscopy after negative staining with uranyl formate (Fig. 5). To facilitate identification of individual FOG molecules on the collagen fibrils FOG was conjugated with 4 nm colloidal gold. Both negative staining (Fig. 5A) and positive staining (Fig. 5B) of collagen fibrils were observed on different locations on the grid, resembling the banding pattern after negative staining with sodium phosphotungstic acid, indicating the polarity of the fibrils (22). On negatively stained fibrils gold-labeled FOG was found at the borders of the more intensely stained gap regions (Fig. 5A). Consistently, binding close to the c_2-band and to the quartet of a-bands of positively stained fibrils was observed (Fig. 5B) (for assignment of the bands see (28)). Evaluation of 300 complexes confirmed the preferential localization of FOG to the border between gap and overlap regions on the collagen fibril (Fig. 5C). A schematic representation (Fig. 5D) corroborates this localization with the binding sites determined on collagen I monomers, in spite of the above mentioned uncertainty to distinguish between NH_2- and COOH-terminal (Fig. 4). Either binding of FOG to the NH_2-terminal of the triple helix, or to the COOH-terminal, together with the corresponding site at 235 nm distance, does in each case result in the observed FOG binding pattern on the striated collagen I fibrils.

GGS expressing FOG bind collagen I in vitro – Eight GGS clinical isolates originating from various infection sites were tested for their ability to bind soluble radiolabeled collagen I. Seven FOG strains bound between 30% and 50% of the added collagen (Fig. 6A). The FOG-deficient isolate G148 bound considerably less collagen I (11%). In experiments with radiolabeled fibronectin, binding of all strains was at a level ($\leq$ 13%) similar to the background of collagen binding by G148 (Fig. 6B). Furthermore, preincubation with fibronectin did not enhance collagen binding to G41 (data not shown). Taken together, these findings demonstrate the specificity of the direct interaction of FOG-expressing GGS with collagen I without requiring fibronectin as a bridging molecule.

GGS expressing FOG adhere to collagen I fibers in the human dermis – The kinetics of primary adhesion of the strains G41 and G148 to human dermis was visualized by scanning electron microscopy. Numbers of bound colonies/mm^2 on dermis thin sections were quantified in the microscope and determined at different time points during two hours. Both strains exhibited a time-dependent adherence, where G41 bound considerably faster than G148. After two hours, adhesion of G41 resulted in a significantly higher density of 1800 colonies/mm^2, as compared to only 200 colonies/mm^2 for strain G148 (Fig. 7A). Preincubating bacteria with soluble collagen I significantly decreased the adhesion of G41, whereas no such effect was observed for G148, emphasizing the specific interaction between G41 and the dermal collagen I network (Fig. 7B).

Next, streptococcal primary adhesion to collagen fibers *in situ* was examined at higher resolution by embedding infected human skin biopsies, followed by ultrathin sectioning and transmission electron microscopy. G41 bacteria intimately associated with cross-striated collagen I fibers in the dermis (Fig. 8A), while G148 bound to a much lesser extent to non-collagenous dermis components (Fig. 8B). The contact between G41 and collagen was mediated by FOG protruding from the surface of G41 as elongated hair-like structures (21). In areas with optimal contrast and resolution these FOG structures were observed bound to the gap regions of the collagen fibrils (Fig. 8A *insert*). This is consistent with the observation that gold-labeled FOG binds to the borders of the gap regions of reconstituted collagen I fibrils *in vitro* (Fig. 5).

GGS expressing FOG adhere to fibrillar collagen I networks in vivo – In order to investigate the *in vivo* relevance of our findings, we allowed streptococci to adhere to collagen I networks of human fibroblasts in monolayer

culture. Scanning electron microscopy showed extensive binding of G41 bacteria to the pericellular collagen matrix (Fig. 9A) as opposed to the considerably weaker binding of G148 (Fig. 9B). These findings were confirmed by determining numbers of colony-forming units (c.f.u.) of adherent bacteria (Fig. 9E, left panel). In further experiments we examined streptococcal primary adhesion in an *in vivo* skin infection model. Balb/c mice received subcutaneous dorsal injections of G41 or G148 streptococci, followed by a 30 min incubation time, which was considered short enough to minimize leukocyte infiltration. Bacterial adherence to the infected areas was examined by scanning electron microscopy and quantified by determination of c.f.u. Colonies of G41 streptococci were frequently associated with the fibrillar collagen I containing networks in the dermis (Fig. 9C). In contrast, G148 bacteria interacted with the dermis to a much lesser extent (Fig. 9D). Similar results were obtained by quantification of GGS adherence by counting c.f.u. of homogenized infected skin areas (Fig. 9E, right panel).

Taken together, our findings demonstrate the specific interaction of the GGS surface protein FOG with the collagen I network of the dermis *in vivo*. This property strongly facilitates primary adhesion of GGS to the host tissue and implies an advantage in pathogenesis of FOG-expressing GGS.

DISCUSSION

The human skin is an important site of entry for GGS infections. In this study we show that the bacterial surface protein FOG is a novel matrix adhesin and virulence determinant, possessing a crucial role for GGS primary adhesion to the human dermis. FOG binds specifically to both collagen I α-chains on two distinct locations of the collagen monomer. Consequently, collagen fibrils provide two binding sites for FOG in the gap-region and serve as substrates for GGS adhesion *in vivo*. This implies that upon skin injury, when the complex collagen matrix in the dermis is exposed, these pathogens can establish primary adhesion to collagen I fibrils in the wound. The immune evasion properties of FOG (21) may facilitate subsequent colonization of the site of infection. Moreover, as collagen I is a ubiquitous constituent of other connective tissues, this collagen is an attractive target for GGS primary adhesion to a variety of locations in the human body.

A recent report describes the ability of GAS to interact with collagen via surface bound fibronectin, resulting in bacterial aggregation and immune evasion (17). The majority of the GAS strains exhibited fibronectin-mediated collagen recruitment, while only a minority showed direct interaction with collagen IV or collagen I. In contrast, our observations demonstrate a direct interaction of GGS with collagen I fibrils *in vivo*. This feature enables GGS to infect human skin without the necessity to recruit bridging molecules, which might not be available at certain infection sites. Examination of eight clinical strains indicates that direct binding to collagen I and comparably low affinity for fibronectin is a common feature among GGS isolates. As all collagen-binding strains express the *fog*-gene, but not strain G148 that does not bind collagen, we assume a general role of FOG in mediating this interaction. This is supported further by the observation that in additional 30 tested clinical isolates PCR products, corresponding to the size of the *fog* gene, were obtained using *fog*-specific primers (21).

Ligand blot experiments combined with MALDI-TOF-MS identification revealed FOG binding to the genetically distinct α-chains of collagen I, in spite of denaturation during SDS-PAGE. This shows that the minimal structural motif essential for the interaction is present in both collagen I α-chains and is independent of the three-dimensional triple helical structure. Binding of FOG to triple helical collagen I, as shown by ligand blot, electron microscopy and surface plasmon resonance, indicates that the assembly of the α-chains into a triple helix does not lead to sterical impairment of the interaction. A binding site for collagen I resides in the NH_2-terminal half of FOG as shown by surface plasmon resonance measurements. Transmission electron microscopy after rotary shadowing suggests that the site of interaction is located at the very NH_2-terminal end of FOG. On collagen I two distinct binding sites were identified. Electron microscopy further indicated an interaction of FOG with collagen I fibrils. Thus, FOG is capable to bind to all different collagen I structures that can occur in severed skin. While binding to the fibrillar collagen network implies a function in dermal adhesion, recruitment of soluble forms of collagen I might contribute to

biofilm formation and might have additional functions in immune evasion.

The finding that FOG-expressing G41 adhere to the collagen matrix of the dermis *in vivo* further emphasizes the importance of this collagen as a target for primary adhesion. It can be expected that further characterization of the FOG-collagen interaction will contribute to understand how sequels of infections with GGS develop. An interesting question is whether FOG behaves promiscuous in its binding to different collagen types. Preliminary data do in fact indicate that this might be the case. This feature could broaden the spectrum of potential GGS infection sites and make the bacteria less dependent on local variations in tissue composition and availability of specific tissue components. In this context it is noteworthy that GAS with rheumatogenic potential has recently been shown to interact with collagen IV. A direct association of the M3 protein and the hyaluronic acid capsule with collagen IV was suggested as a basis for poststreptococcal rheumatic disease (18). An emerging general importance of collagen adhesins as virulence factors is supported by another recent report describing the direct interaction of *Staphylococcus aureus* with collagen II (19). This feature was shown to be mediated by the adhesin CNA and promoted early colonization of joints of mice *in vivo*.

Here we show that once FOG-carrying GGS have passed the epithelium, they possess an efficient mechanism to adhere to and colonize the connective tissue of the host. Comparing the results obtained with GGS strains isolated from different sites of infection did not show a connection between the ability to bind collagen I and to the site of infection. The observation is consistent with the wide tissue distribution of the matrix protein. Factors that might determine the tissue specificity of different GGS strains remain to be discovered. The processes leading from colonization to development of pathological GGS infections are not fully understood yet. Age and underlying diseases, like diabetes, or injury (burn, chronic ulcer) are common risk factors for the host. Apparently, a particular susceptibility of those patients depends on impaired immunity, possibly in combination with the circumvention or loss of the protective epithelium. The pathogenesis of GGS infections is also determined by the evolved bacterial modes of immune evasion, acquisition of nutrients, or dissemination. The interaction described in this work probably contributes to those additional mechanisms of pathogenesis, which motivates further investigations.

REFERENCES

1. Oster, H., and Bisno, A.L. (2000) *Gram-Positive Pathogens*, (Fischetti, V.A., Novick, R.P., Ferretti, J.J., Portnoy, D.A., and Rood, J.I., eds.), American Society for Microbiology, Washington, D.C., 184-190

2. Haidan, A., Talay, S.R., Rohde, M., Sriprakash, K.S., Currie, B.J., and Chhatwal, G.S. (2000) *Lancet*. **356**, 1167-1169

3. Auckenthaler, R., Hermans, P.E., and Washington, J.A., 2nd (1983) *Rev. Infect. Dis.* **5,** 196-204

4. Nohlgard, C., Bjorklind, A., and Hammar, H. (1992) *Acta Derm. Venerol.* **72**, 128-130

5. Sylvetsky, N., Raveh, D., Schlesinger, Y., Rudensky, B., and Yinnon, A.M. (2002) *Am. J. Med.* **112**, 622-626

6. Cunningham, M.W. (2000) *Clin. Microbiol. Rev.* **13**, 470-511

7. Courtney, H.S., Hasty, D.L., and Dale, J.B. (2002) *Ann. Med.* **34**, 77-87

8. Beachey, E. H., and Ofek, I. (1976) *J. Exp. Med.* **143**, 759-71

9. Courtney, H.S., von Hunolstein, C., Dale, J.B., Bronze, M.S., Beachey, E.H., and Hasty, D.L. (1992) *Microb. Pathog.* **12**, 199-208

10. Hasty, D.L., Ofek, I., Courtney, H.S., and Doyle, R.J. (1992) *Infect. Immun.* **60**, 2147-52

11. Molinari, G., Talay, S.R., Valentin-Weigand, P., Rohde, M., and Chhatwal, G.S. (1997) *Infect. Immun*. **65**, 1357–1363

12. Jadoun, J., Ozeri, V., Burstein, E., Skutelsky, E., Hanski, E., and Sela, S. (1998) *J. Infect. Dis*. **178**, 147–158

13. Fluckiger, U., Jones, K.F., and Fischetti, V.A. (1998) *Infect. Immun*. **66**, 974–979.

14. Ozeri, V., Rosenshine, I., Mosher, D.F., Fässler, R., and Hanski, E. (1998) *Mol. Microbiol*. **30**, 625-637

15. Cue, D., Southern, S.O., Southern, P.J., Prabhakar, J., Lorelli, W., Smallheer, J.M., Mousa, S.A., and Cleary, P.P. (2000) *Proc. Natl. Acad. Sci. U S A* **97**, 2858-2863

16. Cue, D., Dombek, P.E., Lam, H., and Cleary, P.P. (1998) *Infect. Immun.* **66**, 4593-4601

17. Dinkla, K., Rohde, M., Jansen, W.T., Carapetis, J.R., Chhatwal, G.S., and Talay, S.R. (2003a) *Mol. Microbiol.* **47**, 861-869

18. Dinkla, K., Rohde, M., Jansen, W.T., Kaplan, E.L., Chhatwal, G.S., and Talay, S.R. (2003b) *J. Clin. Invest.* **111**, 1905-1912

19. Xu, Y., Rivas, J.M., Brown, E.L., Liang, X., and Höök, M. (2004) *J. Infect. Dis.* **15**, 2323-2333

20. Kline, J.B., Xu, S., Bisno, A.L., and Collins, C.M. (1996) *Infect. Immun*. **64**, 2122-2129

21. Johansson, H.M., Mörgelin, M., and Frick, I.-M. (2004) *Microbiology* **150**, 4211-4221

22. Björck, L., and Kronvall, G. (1984) *J. Immunol.* **133**, 969-974

23. Zhang, W. and Chait, B.T. (2000) *Anal. Chem.* **72**, 2482-2489

24. Frick, I.M., Mörgelin, M., and Björck, L. (2000) *Mol. Microbiol*. **37**, 1232-1247

25. Mould, P., Holmes, D., Kadler, K. and Chapman, J. (1985) *J. Ultrastr. Res*. **91**, 66-7625

26. Baschong, W. and Wrigley, N.G. (1990) *J Electron Microsc Tech*. **14**, 313-23

27. Roth, J., Bendayan, M., and Orci, L. (1980). *J. Histochem. Cytochem.* **26**, 1074-1081

28. Kadler, K.E., Holmes, D.F., Trotter, J.A., and Chapman, J.A. (1996) *Biochem. J.* **316**, 1-11

FOOTNOTES

∗We are grateful to Maria Baumgarten for excellent technical assistance. Skin biopsies were a kind gift of Dr. Artur Schmitdchen, to whom we are indebted. We thank Rita Wallén and Erik Hallberg (Department of Functional Morphology, Lund University) for helpful discussions and practical advice with electron microscopy. We thank Dr. Lars Björck for valuable discussions. This work was supported by the Swedish Research Council (project 7480), the Crafoordska, Magnus Bergvall, Greta & Johan Kocks, Tore Nilsson, and Alfred Österlund foundations, the Royal Physiographic Society and Hansa Medical AB. D.P.N. was supported by the Anna Greta Crafoord Foundation.

FIGURE LEGENDS

Fig. 1. Colonization of human dermis by GGS. The FOG expressing strain G41 (left panel) and the FOG deficient strain G148 (right panel) were tested for adhesion to sections of human skin (A and B) and colonization of human skin biopsies (C and D). For light microscopy bacteria (arrowheads) were visualized by binding of HRP-conjugated IgG, followed by staining with DAB (A) or H&E (C). In parallel, samples were visualized by scanning electron microscopy (B and D). Arrowheads point at GAS colonies. Bars represent 20 μm in A and C and 5 μm in B and D. The insert in D shows G41 attached to fibers of the dermis. The bar represents 2.5 μm in the insert.

Fig. 2. Binding of radiolabeled FOG 1-C to human skin extracts. (A) Human skin extract (lane 1 and 3) and calf skin collagen I (lane 2 and 4) were analyzed by SDS-PAGE. One gel was stained with Coomassie (stain) and the other gel was transferred to a PVDF membrane (blot) and incubated with radiolabeled FOG 1-C. M_r-standards, origin, and front (arrows) of the separating gel are indicated to the left. Indicated are also α1-, α2-chain, β-, and γ-fragments of collagen I. Numbers a, b and c indicate the mobility of dermis components that interact with FOG and were then analyzed by MALDI-TOF-MS. (B) Collagen I denatured in a solution of 4 M guanidine hydrochloride (+) and non-denatured collagen I (-) were applied in slots to a PVDF membrane and incubated with radiolabeled FOG 1-C. The amount of applied collagen I is indicated to the right.

Fig. 3. Surface plasmon resonance measurements - (A) FOG, (B) FOG 1-C (C) FOG 1-B and (D) GST were injected into the Biacore system. Injection started at t = 0 s. Curves represent the difference between the signals of a surface coupled with collagen I and a control surface. The signal is corrected by subtracting the buffer signal. (E) A schematic representation of the FOG-molecule with its domains is shown. Indicated below are fragments FOG 1-C and FOG 1-B. Numbers refer to the amino acid residue positions where 1 is the first residue of the mature protein. (F) The recombinant fusion proteins with GST were visualized by transmission electron microscopy after rotary shadowing. A panel of selected molecules shows, in duplicate and from left to right, FOG, FOG 1-C, FOG 1-B, and GST. Average lengths +/- S.D. of the different constructs are given in the Figure. The bar in F corresponds to 50 nm.

Fig. 4. Electron microscopy of FOG-collagen I complexes. An overview (A) and a panel of selected particles (B) show complexes of FOG and collagen I. The bars represent 200 nm in (A) and 100 nm in (B). A histogram (C) demonstrates the sites of interaction. The collagen triple helix was subdivided into 5 nm intervals. The relative frequency (N/N_0) denotes the fraction of interacting FOG molecules that bound within this interval.

Fig. 5. Binding of FOG to collagen I fibrils. Interaction of gold labeled FOG with in vitro constituted collagen I fibrils was visualized after staining with uranyl formate. Areas of negative staining (A) and positive staining (B) were examined by transmission electron microscopy. The schematic illustrations in (C) and (D) are aligned with the banding pattern of the fibrils in (A) and (B). Ticks indicate the borders between alternating gap (g) and overlap (o) regions. In (D) the staggered arrangement of collagen I monomers in a fibril is schematically illustrated. The hypothetical distribution of FOG binding positions on the collagen I molecule is depicted below. The NH_2- and COOH-terminals of the molecules are denoted N and C, respectively. The bar represents 100 nm.

Fig. 6. Collagen I recruitment by GGS. Binding of ^{125}I-labeled collagen I (A) and fibronectin (B) to different GGS isolates is presented as percentage of the bound radioactive protein. Error bars indicate the mean standard error.

Fig. 7. Kinetics of primary adhesion of GGS to human dermis. (A) Time-dependence of the primary adhesion of G41 and G148 was determined by counting the number of bound bacterial colonies per mm^2 dermis in the scanning electron microscope. (B) Strain G41 (1 and 2) and G148 (3 and 4) were allowed to adhere for 1 h to the skin sections in absence (1 and 3) or presence (2 and 4) of soluble collagen I.

Fig. 8. Infection of human dermis *ex vivo*. Ultra thin sections of skin biopsies infected with (A) G41 or (B) G148 are shown. A site of contact between G41 and a collagen I-containing fiber is shown with

higher magnification (insert). Open arrowheads point at contacts between the collagen fibril and structures protruding from the streptococcal surface.

Fig. 9. Streptococcal primary adhesion *in vivo*. Monolayers of human fibroblasts with their pericellular matrix were infected with G41 (A) or G148 (B) and visualized by scanning electron microscopy. (C) Scanning electron microscopy of G41 and G148 (D) adhered to the dermis of mice. Left panel: electron micrographs; right panel: image processing in pseudocolour to present bound bacteria with enhanced contrast. (E) Primary adhesion of G41 and G148 streptococci to human foreskin fibroblasts (left panel) and the dermis of Balb/c mice (right panel) was quantified by counting numbers of c.f.u.

TABLE I

Table I: Analysis of Peptide Mass Fingerprints

Band	Rank	Estimated Z	Description	Assignment[a]
1	1	1.78	collagen I α1-chain	
	2	0.69	collagen I α2-chain	collagen I α2-chain
2	1	2.11	collagen I α1-chain	collagen I α1-chain
3	1	1.94	collagen I α1-chain	
	2	0.45	collagen I α2-chain	collagen I β-fragment

[a] based on comparison with purified collagen I from calf skin in SDS-PAGE

Fig. 1

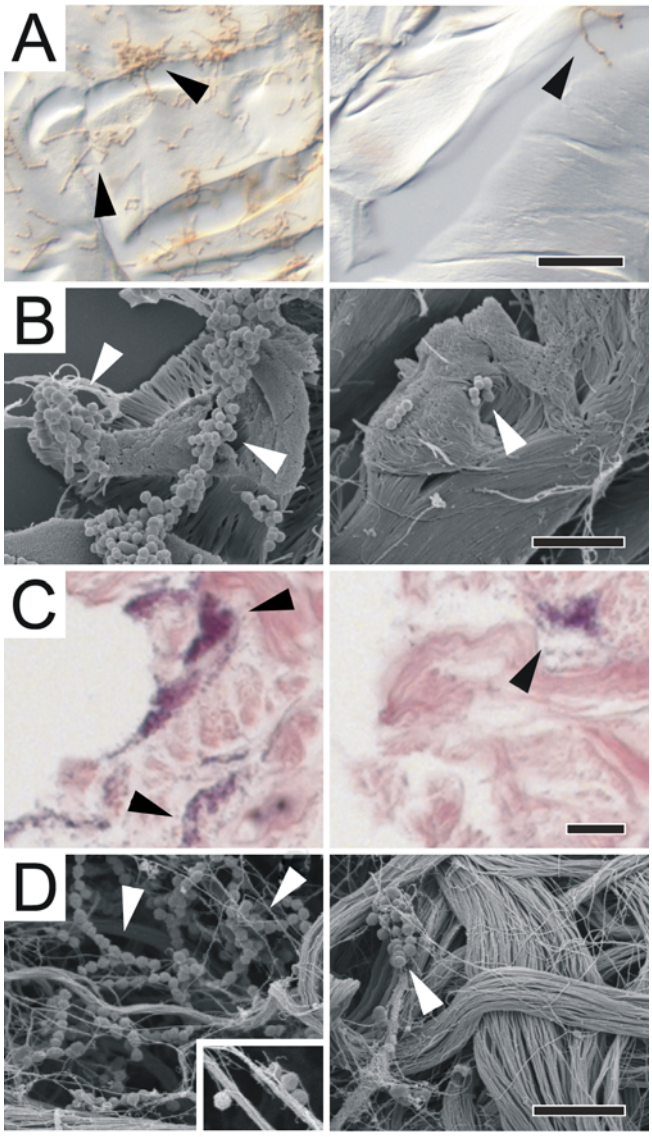

Nitsche et al.

Fig. 2

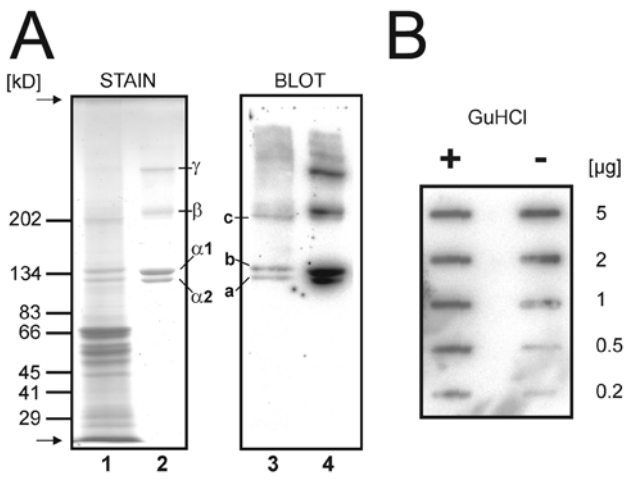

Nitsche et al.

Fig. 3

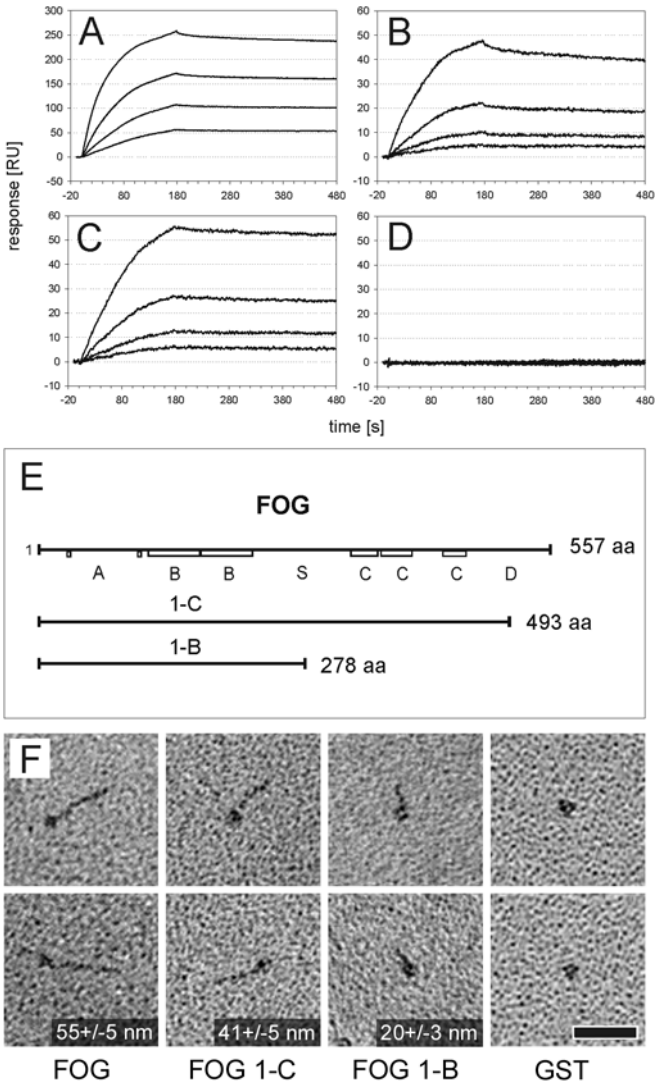

Nitsche et al.

Fig. 4

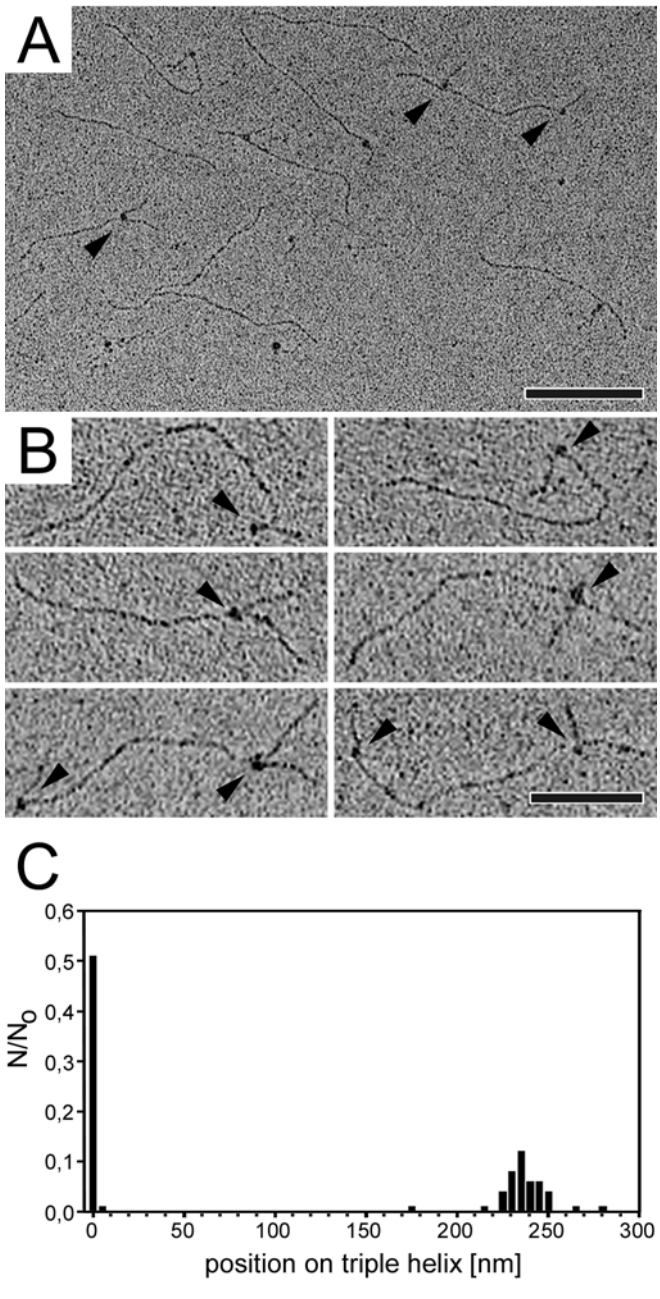

Nitsche et al.

Fig. 5

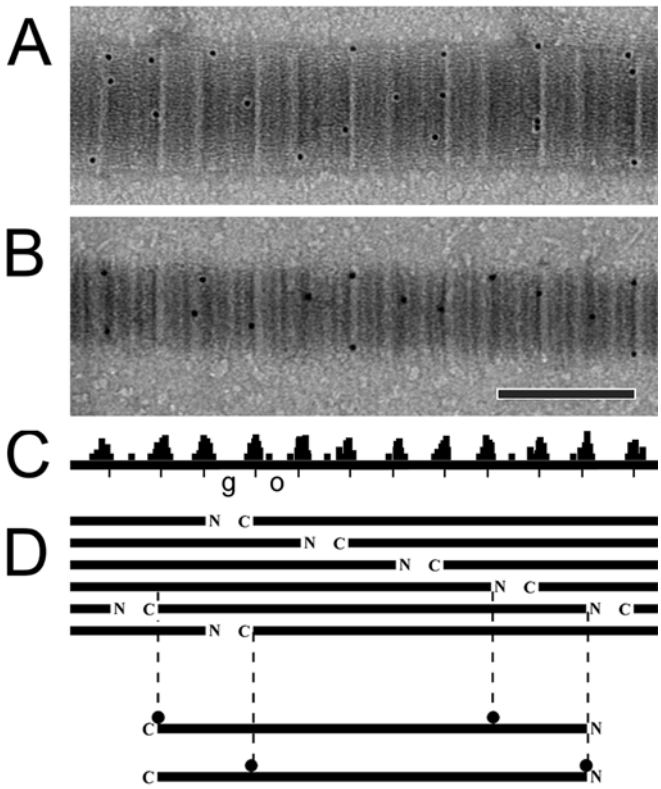

Nitsche et al.

Fig. 6

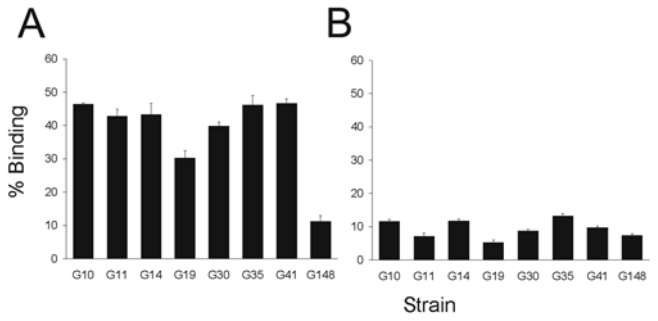

Nitsche et al.

Fig. 7

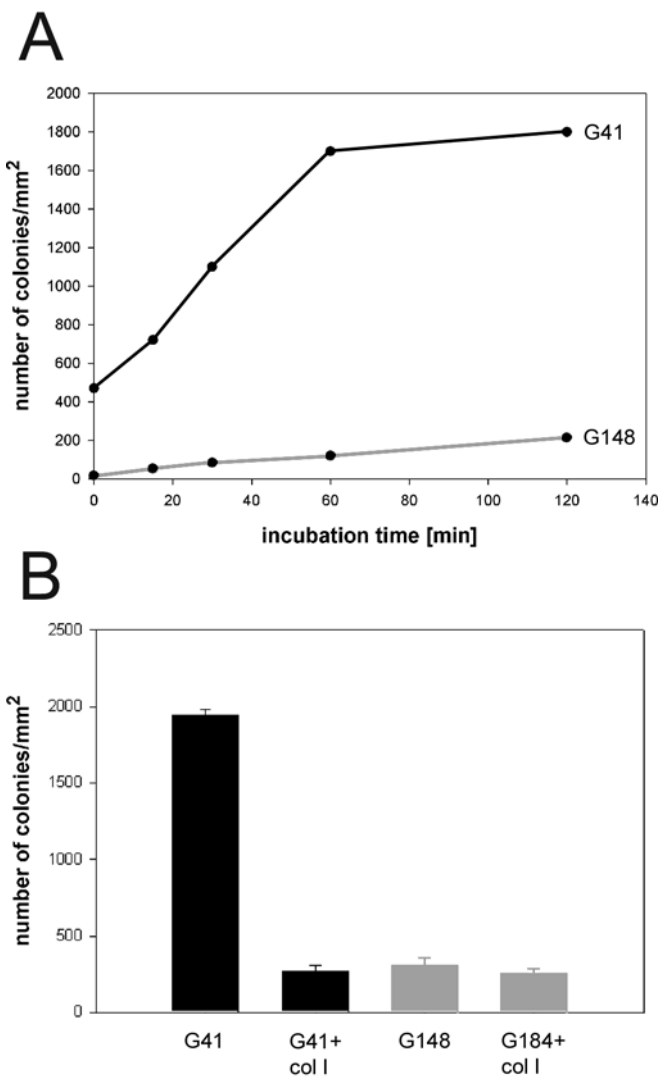

Nitsche et al.

Fig. 8

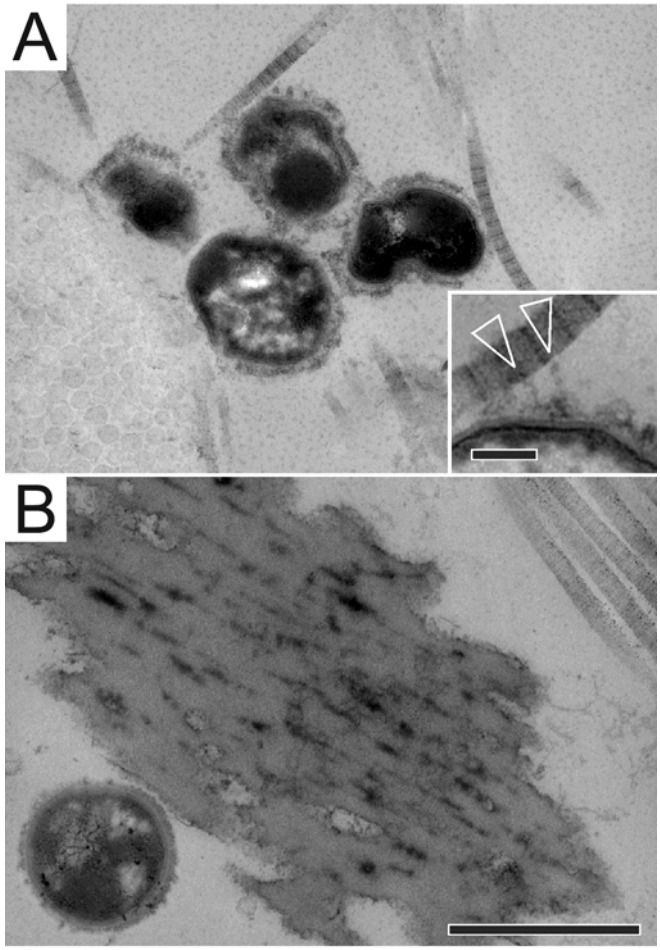

Nitsche et al.

Fig. 9

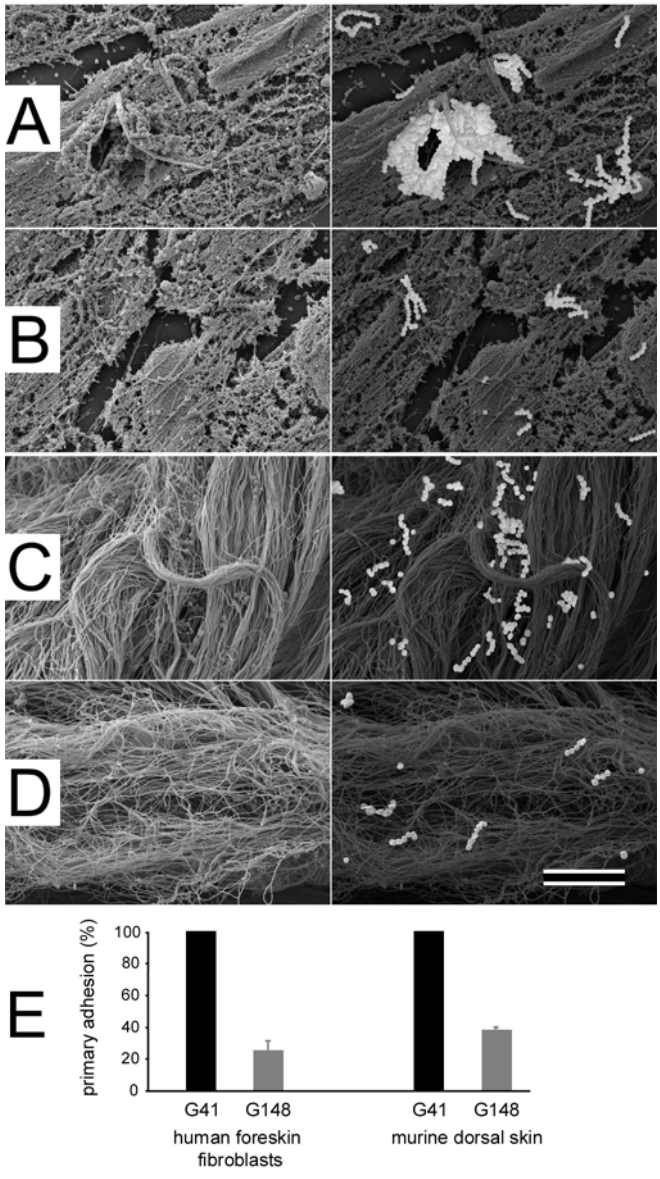

Nitsche et al.